Strain-induced insulator-to-metal transition in LaTiO₃ within DFT + DMFT

Krzysztof Dymkowski[*] and Claude Ederer[†]

Materials Theory, ETH Zürich, Wolfgang-Pauli-Strasse 27, 8093 Zürich, Switzerland
(Received 20 November 2013; revised manuscript received 19 March 2014; published 14 April 2014)

We present results of combined density functional theory plus dynamical mean-field theory (DFT + DMFT) calculations, which show that the Mott insulator LaTiO₃ undergoes an insulator-to-metal transition under compressive epitaxial strain of about −2%. This transition is driven by strain-induced changes in the crystal-field splitting between the Ti t_{2g} orbitals, which in turn are intimately related to the collective tilts and rotations of the oxygen octahedra in the orthorhombically distorted $Pbnm$ perovskite structure. An accurate treatment of the underlying crystal structure is therefore crucial for a correct description of the observed metal-insulator transition. Our theoretical results are consistent with recent experimental observations and demonstrate that metallic behavior in heterostructures of otherwise insulating materials can emerge also from mechanisms other than genuine interface effects.

Emergent phenomena at oxide interfaces are currently attracting a lot of attention both from basic science as well as due to their prospects for future technological devices [1–3]. Oxide heterostructures often exhibit properties that are not present in the individual materials. For example, metallic conductivity has been observed in heterostructures consisting of ultrathin layers of LaTiO₃ (1–4 unit cells thick) embedded in SrTiO [4], even though the corresponding bulk materials are both insulators. This has been explained by charge transfer between the Ti^{3+} and Ti^{4+} cations at the interfaces between the two components [5,6]. However, more recently, metallicity has also been found in thin films of LaTiO₃ (15-45 nm thick) grown epitaxially on SrTiO₃ [7,8]. It has been shown that the sheet carrier density in these films scales linearly with film thickness, which suggests that the metallicity is not just restricted to the interface region. Furthermore, a comparison of LaTiO₃ films grown on different substrates, suggests that the metallic properties are controlled by substrate-induced epitaxial strain [7].

To better understand the physical mechanisms behind emerging properties in oxide heterostructures, it is important to clearly distinguish the effects of different factors, such as e.g., strain, defects, structural and electronic reconstruction at the interface, etc. Here, we present results of first-principles calculations using a combination of density functional theory and dynamical mean-field theory (DFT + DMFT) [9–12], assessing specifically the effect of epitaxial strain on LaTiO₃, independent from interface effects or variations in defect concentration. We find that compressive epitaxial strain can indeed induce a metal-insulator transition, consistent with the experimental observations, whereas tensile strain strongly enforces the insulating character. Furthermore, we show that this behavior is controlled mainly by strain-induced changes in the crystal-field splitting within the Ti t_{2g} bands.

Bulk LaTiO₃ at room temperature is a paramagnetic Mott insulator [13,14]. The theoretical description of such systems is challenging, since the standard local density or generalized gradient approximations are not suitable for describing the Mott-insulating state without any symmetry-breaking long-range order [9]. However, a good description of LaTiO₃ and other perovskite systems with d^1 electron configuration of the transition metal cation can be achieved within the DFT + DMFT approach [15–17]. Using this method, it has been shown that the Mott-insulating character of d^1 perovskites with $Pbnm$ symmetry, such as LaTiO₃ [18,19], is controlled by the amplitude of the characteristic structural distortion, i.e., tilts of the oxygen octahedra, the so-called GdFeO₃-type distortion [see Figs. 1(b) and 1(c)] [15].

On the other hand, first-principles calculations for a number of $Pbnm$ perovskites have shown that epitaxial strain generally affects both character and amplitude of the octahedral tilts (see Ref. [20] for a review). Since, as stated above, the insulating character of LaTiO₃ is controlled by the octahedral tilts, it can be expected that epitaxial strain will have a pronounced effect on the electronic properties of LaTiO₃ and eventually even drive the system towards a metallic state. Conversely, in order to understand the effect of epitaxial strain on LaTiO₃, it is thus very important to correctly account for the resulting changes in the octahedral tilt distortion.

We therefore start by performing accurate structural relaxations for LaTiO₃ under different epitaxial constraints in the following way. We fix the two "in-plane" lattice constants to $a = b = (\epsilon + 1)a_0$, where the value $a_0 = 5.60$ Å corresponds to the "coherent structure" [20], i.e. minimal energy under the constraint $a = b$. For each strain ϵ we then relax the "out-of-plane" lattice constant c and all internal structural parameters (for simplicity we assume that the films grow with the orthorhombic c direction (long axis) perpendicular to the substrate plane). All structural relaxations are performed within the generalized gradient approximation (GGA) [21] to density functional theory (DFT) using the QUANTUM ESPRESSO code [22] with a plane-wave basis and ultrasoft pseudopotentials [23]. Since our work focuses on the room-temperature paramagnetic phase of LaTiO₃, all calculations are performed for the non-spin-polarized case. Further technical details can be found in Ref. [24].

We note that the octahedral tilt distortion in perovskites is assumed to be driven by the size ratio between the two different cations [25] as well as by hybridization between the oxygen anions and the large A-site cation [15]. These

---
[*]krzysztof.dymkowski@mat.ethz.ch
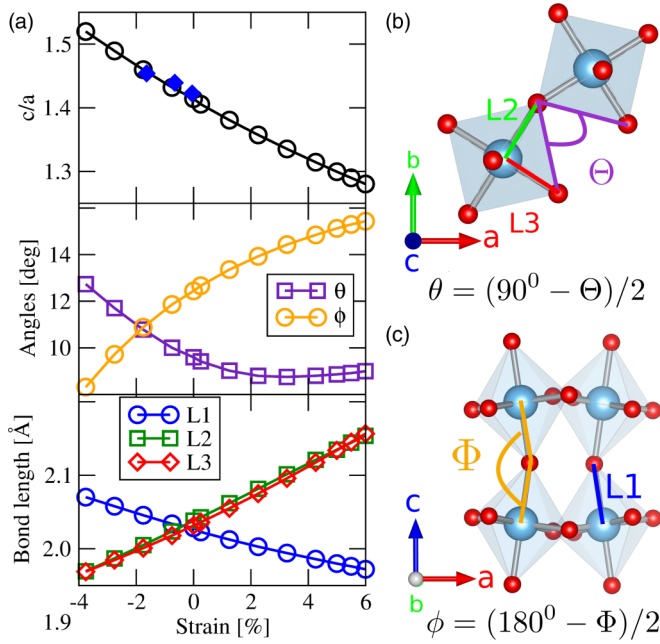[†]claude.ederer@mat.ethz.ch

FIG. 1. (Color online) (a) Calculated c/a ratio (top), octahedral tilt angles (middle), and Ti-O bond distances (bottom) in LaTiO$_3$ as a function of in-plane strain. The c/a ratio is calculated from the orthorhombic lattice parameters ($c/a \approx \sqrt{2}$ for zero strain) and is compared to experimental data from Ref. [7] (filled diamonds). (b) and (c) show projections of the orthorhombically distorted $Pbnm$ perovskite structure. The three different Ti-O bond distances are denoted as L1–L3. The angles θ and ϕ measure in-plane "rotations" and out-of-plane "tilts," respectively, and are related to specific bond angles, which are indicated in (b) and (c) by capital letters Θ and Φ.

effects are generally well described within GGA. Thus an accurate treatment of electronic correlations is not necessary to describe the structural properties of LaTiO$_3$. Nevertheless, in order to benchmark the accuracy of our calculated structural parameters, we first perform a full unconstrained structural relaxation of the orthorhombic $Pbnm$ bulk structure. All calculated lattice parameters agree well with available experimental data. In particular, the octahedral tilt angles deviate by less than 1° from the experimental values (see Ref. [24] for more details).

We now discuss the results of our structural relaxations under epitaxial strain. Figure 1(a) shows the calculated c/a ratio, the octahedral tilt angles, and the Ti-O bond distances as a function of applied strain. As expected, compressive (tensile) strain results in an elongation (reduction) of c. The calculated c/a shows good agreement with experimental data from Ref. [7]. Furthermore, it can be seen that epitaxial strain has a pronounced effect on the octahedral tilt angles as well as on the Ti-O bond distances. The octahedral tilt angles show the expected behavior, similar to what has been observed in other $Pbnm$ perovskites [20]. The in-plane "rotations," characterized by the angle θ, increase under compressive strain, in order to decrease the unit cell area within the a-b plane. On the other hand, the out-of-plane "tilts," characterized by ϕ, decrease due to the elongation along c, which straightens out the Ti-O-Ti bonds along this direction. Tensile strain

leads to the opposite trends. When looking at the Ti-O bond distances, it can be seen that all three bond distances are nearly equal for the unstrained structure, i.e., there is no significant Jahn-Teller distortion of the oxygen octahedra. Under strain, the lengths of the two "in-plane" bonds (L2/L3) remain approximately equal and are reduced (elongated) for compressive (tensile) strain. The bond distance along c (L1) exhibits the opposite trend.

Thus, while the octahedral tilt angles follow the trends expected for a network of rigid octahedra under strain, the octahedra are in fact not completely rigid and also deform as a result of the applied strain. Part of the strain is therefore compensated by changes in the octahedral tilt angles and part of it is compensated by the deformation of the octahedra. The deviation from the behavior of rigid octahedra is especially pronounced for large tensile strain ($\sim$4–6%) where the angle θ becomes nearly constant and even shows a slight increase with increasing strain [see Fig. 1(a)].

After analyzing the structural changes under strain, we now turn to the electronic properties. Following previous work [15–17], we employ a DMFT treatment to account for the electron-electron interaction within the partially filled bands around the Fermi energy with predominant Ti t_{2g} character. We express the Kohn-Sham Hamiltonian in a basis of maximally localized Wannier functions [26,27] describing the effective Ti t_{2g} bands, and use this as the noninteracting part H_0 of a multiband Hubbard Hamiltonian $H = H_0 + H_{int}$. The local electron-electron interaction H_{int} is expressed in the Slater-Kanamori form, including both spin-flip and pair hopping terms, with the parameters U and J describing the intra-orbital Coulomb interaction and Hund's rule coupling, respectively (see, e.g., Ref. [28]). The local Green's function is then calculated within DMFT [9] at temperature $T = 1/(k_B\beta)$ using a continuous time hybridization expansion quantum Monte Carlo solver [29] implemented in the TRIQS 0.9 code [30]. Off-diagonal elements between different orbitals on the same site are taken into account both for the local Green's functions and the self-energy. Such off-diagonal elements appear due to the symmetry-lowering associated with the octahedral tilts. No sign problem related to these off-diagonal elements was encountered in the Monte Carlo calculations. All calculations are performed for $\beta = 40$ eV^{-1} ($T = 290$ K) and $J = 0.64$ eV, while U is varied between 4 and 5.9 eV. More details can be found in Ref. [24].

Figure 2 shows the trace of the local Green's function at imaginary time $\tau = \beta/2$ as a function of U [31], calculated for different strain values. Based on the relation
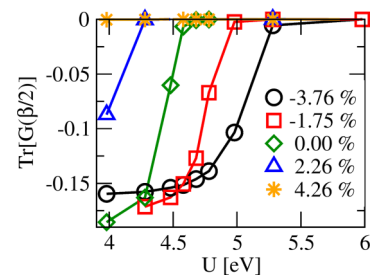

FIG. 2. (Color online) Trace of the local Green's function at $\tau = \beta/2$ as function of the interaction parameter U, calculated for different values of epitaxial strain.

$A(\omega = 0) = -\frac{1}{\pi} \lim_{\beta \to \infty} \beta G(\beta/2)$, this can be taken as a measure of the total spectral function at the Fermi level (see, e.g., Ref. [28]). It can be seen that there is a change from $\mathrm{Tr}\, G(\beta/2) \neq 0$ to $\mathrm{Tr}\, G(\beta/2) \approx 0$ in the interval $4\,\mathrm{eV} < U < 5.5\,\mathrm{eV}$ for all negative strain values, i.e., the system undergoes a metal-insulator transition with increasing U. It can further be seen that epitaxial strain has a pronounced effect on the critical U for this transition. While tensile strain strongly decreases the critical U (to values smaller than 4 eV for $\epsilon > 2.26\%$), compressive strain has the opposite effect, and increases the critical U to slightly above 5 eV at -3.76% strain. Thus compressive (tensile) strain favors the metallic (insulating) state.

Thus, irrespective of any uncertainty regarding the appropriate value of U and possible small inaccuracies in the calculated GGA lattice parameters, our calculations clearly show that compressive strain promotes metallicity in $LaTiO_3$, consistent with the experimental observation of metallic conductivity in thin films of compressively strained $LaTiO_3$ [7]. Assuming a realistic U for the Ti t_{2g} Wannier orbitals in the range of 4.5–5 eV, our results show that a strain-induced insulator-to-metal transition occurs for compressive strains around -2%, which compares well with the lattice mismatch of -1.6% for $LaTiO_3$ films grown on $SrTiO_3$. Of course our calculations do not exclude the possibility that other aspects such as oxygen vacancies or interface polarity can also strongly influence the conductivity of the $LaTiO_3$ films.

We now analyze the strain-induced transition in more detail by looking at the occupations and energy levels of the three individual t_{2g} orbitals. Figure 3 shows the eigenvalues of the occupation matrix $n_{mm'} = -\sum_\sigma G^\sigma_{mm'}(\beta)$ together with the "crystal-field levels" of the effective Ti t_{2g} Wannier functions. The latter are obtained by diagonalizing the local on-site Hamiltonian H_0. We have verified that the resulting "crystal field basis" is very similar to the basis diagonalizing the local occupation matrix (the scalar product between the eigenvector corresponding to the lowest crystal-field orbital and the eigenvector corresponding to the "nearly-filled" orbital is larger than 0.96 for all strain values).

It can be seen from Fig. 3(a) that in the unstrained state one orbital is lower in energy by 108 meV compared to the other two t_{2g} states, whereas the splitting between the two energetically higher orbitals is rather small (26 meV). This is consistent with the orbital splittings calculated in Ref. [17] for bulk $LaTiO_3$. We point out that this crystal-field splitting is a result of the octahedral rotations, which lower the symmetry of the Ti sites to triclinic, whereas the Ti-O bond distances are essentially equal along all three directions [see Fig. 1(a)]. Tensile strain conserves the energetic order between the t_{2g} orbitals, i.e., one orbital at lower energy and two nearly degenerate levels at higher energies, and strongly increases the corresponding splitting. In contrast, compressive strain removes the near degeneracy between the two orbitals with higher energy, while reducing the splitting between the lowest and the intermediate energy level to 65 meV at a compressive strain of -3.76%. Thus applying strain does not simply increase the overall crystal-field splitting but leads to qualitative changes in the relative energy differences between the three Ti t_{2g} Wannier orbitals.

The changes in the crystal-field levels are mirrored in the orbital occupations calculated within DMFT [see Fig. 3(b)]. For
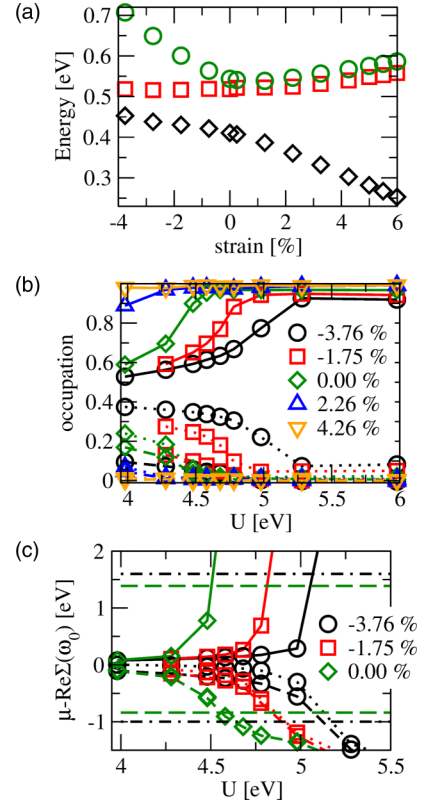

FIG. 3. (Color online) (a) Strain dependence of the three "crystal-field levels" corresponding to the effective Ti t_{2g} Wannier orbitals. (b) and (c) Occupations and "effective" chemical potential $\mu - \mathrm{Re}\,\Sigma(\omega_0)$, respectively, as a function of the interaction parameter U, calculated for different strain values. The three different orbitals for each strain are indicated by solid, dotted, and dashed lines, in order of decreasing occupation. The dashed and dot-dashed horizontal lines in (c) indicate the band-edges of the noninteracting system for 0% and 3.76% strain, respectively. In (a) and (c), the Fermi level was used as zero energy reference for each strain value.

large tensile strain the energetically lowest orbital is essentially completely filled, whereas the other two orbitals remain empty. With increasing compressive strain one of the two empty orbitals gains some occupation at the expense of the filled orbital. This trend can clearly be seen from the occupations for large U, i.e., where the system is insulating. The transition to the metallic phase is then accompanied by a strong charge transfer from the "nearly filled" into the "nearly empty" orbital, while the third orbital remains mostly unaffected.

It thus appears that the decrease of the splitting between the two lowest crystal-field levels under compressive strain is crucial to facilitate the metallic state in $LaTiO_3$. In contrast, tensile strain strongly increases this crystal-field splitting and thus enforces the insulating state, i.e., the critical U for the transition is strongly reduced (see Fig. 2). This is further evidenced by the orbitally resolved real part of the self-energy at zero frequency, which can be viewed as an additional "effective" chemical potential shift (see, e.g., Ref. [32]). As can be seen from Fig. 3(c), where $\Sigma(0)$ has been approximated by its value at the lowest Matsubara frequency, the electron-electron interaction strongly enhances the splitting between the energetically lowest and the two higher lying orbitals
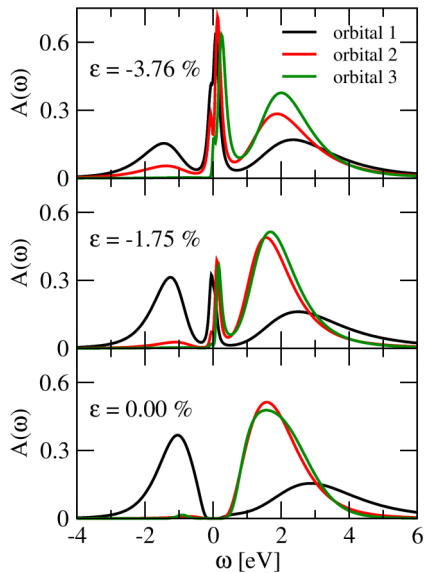
FIG. 4. (Color online) Orbitally resolved spectral functions for $U = 4.78$ eV and $\epsilon = 0$ (bottom), $\epsilon = -1.75\%$ (middle), and $\epsilon = -3.76\%$ (top). Orbitals 1, 2, and 3 correspond to the eigenfunctions of the occupation matrix and are ordered with decreasing occupation.

in the insulating regime and effectively shifts the chemical potential beyond the boundaries of the noninteracting bands [32]. It can also be seen from Fig. 3(c) that on the other hand the t_{2g} bandwidth is only weakly affected by epitaxial strain. This is a consequence of two competing effects on the dominant nearest neighbor hopping amplitudes: the shorter Ti-O bond distances within the a-b plane under compressive strain would in principle lead to an increase in hopping, on the other hand the greater distortion of the corresponding Ti-O-Ti bond angle has exactly the opposite effect (see Ref. [24] for more details). This suggests that the tendency towards the metallic phase under compressive strain is mainly controlled by strain-induced changes in the crystal-field energies, which are strongly enhanced due to the electron-electron interaction.

Finally, in Fig. 4, we present orbitally resolved spectral functions for different strain values and $U = 4.78$ eV. The spectral functions are obtained from the imaginary time Green's functions by analytic continuation using the maximum entropy method [33] (see also Ref. [24]). The spectral functions obtained in the insulating state for zero strain agree well with those reported in Ref. [17] for bulk LaTiO$_3$. All spectral weight below zero energy corresponds to the occupied orbital with lowest energy. With increasing compressive strain the systems becomes metallic

and strong quasiparticle features appear around zero energy for all three orbitals, consistent with Tr $G(\beta/2) \neq 0$ shown in Fig. 2. Nevertheless, orbital 3 has negligible spectral weight at negative energies for all strain values.

In summary, our calculations demonstrate an insulator-to-metal transition under compressive epitaxial strain in LaTiO$_3$, consistent with recent reports of metallic conductivity in LaTiO$_3$ films grown on SrTiO$_3$. The origin of this transition is the reduced crystal-field splitting under compressive strain, which facilitates electron transfer between the two lowest Ti t_{2g} levels. In contrast, the increase of this splitting under tensile strain leads to a strong reduction of the critical U for the insulating state, which suggests that the insulating character of LaTiO$_3$ could be enhanced by growing it on substrates with slightly larger lattice constants. We note that, while additional interface effects or the presence of defects might further influence the properties of the real system, our results indicate that such effects are not essential for explaining the observed metallic behavior.

The fact that strain can alter the delicate balance between electron hopping and Coulomb interaction and destroy the Mott insulating state in LaTiO$_3$, has been previously suggested [34]. However, the corresponding calculations were performed for a simplified tetragonal crystal structure without octahedral tilts. Our results demonstrate the close interplay between structure and electronic properties in LaTiO$_3$ and also show that it is crucial to consider realistic crystal structures within DMFT calculations.

It is clear that epitaxial strain is an important factor for the emerging properties observed in oxide heterostructures. Therefore, in order to understand the effect of the interface in these heterostructures, the properties of the corresponding strained material should be taken as reference, not the properties of the bulk material. Interface effects can then successively be introduced using slab supercells. For example, a fully self-consistent DFT + DMFT study of short period LaTiO$_3$-SrTiO$_3$ multilayer-structures, including full structural relaxation of the unit cell, has been presented recently [35]. While no detailed analysis of the origin of the metallicity (e.g., strain versus interface effects) or of the degree of octahedral tilts has been presented, Ref. [35] demonstrates the feasibility of such calculations even for complex multilayer structures with large unit cells.

[1] J. Mannhart and D. G. Schlom, Science **327**, 1607 (2010).

[2] J. Chakhalian, A. J. Millis, and J. Rondinelli, Nat. Mater. **11**, 92 (2012).

[3] H. Y. Hwang, Y. Iwasa, M. Kawasaki, B. Keimer, N. Nagaosa, and Y. Tokura, Nat. Mater. **11**, 103 (2012).

[4] A. Ohtomo, D. A. Muller, J. L. Grazul, and H. Y. Hwang, Nature (London) **419**, 378 (2002).

[5] S. Okamoto and A. J. Millis, Nature (London) **428**, 630 (2004).

[6] S. Okamoto, A. J. Millis, and N. A. Spaldin, Phys. Rev. Lett. **97**, 056802 (2006).

[7] F. J. Wong, S.-H. Baek, R. V. Chopdekar, V. V. Mehta, H.-W. Jang, C.-B. Eom, and Y. Suzuki, Phys. Rev. B **81**, 161101 (2010).

[8] C. He, T. D. Sanders, M. T. Gray, F. J. Wong, V. V. Mehta, and Y. Suzuki, Phys. Rev. B **86**, 081401 (2012).

[9] A. Georges, G. Kotliar, W. Krauth, and M. J. Rozenberg, Rev. Mod. Phys. **68**, 13 (1996).

[10] V. I. Anisimov, A. I. Poteryaev, M. A. Korotin, A. O. Anokhin, and G. Kotliar, J. Phys.: Condens. Matter **9**, 7359 (1997).

[11] G. Kotliar and D. Vollhardt, Phys. Today **3**, 53 (2004).

[12] K. Held, Adv. Phys. **56**, 829 (2007).

[13] A. Fujimori, I. Hase, H. Namatame, Y. Fujishima, Y. Tokura, H. Eisaki, S. Uchida, K. Takegahara, and F. M. F. de Groot, Phys. Rev. Lett. **69**, 1796 (1992).

[14] T. Arima, Y. Tokura, and J. B. Torrance, Phys. Rev. B **48**, 17006 (1993).

[15] E. Pavarini, S. Biermann, A. Poteryaev, A. I. Lichtenstein, A. Georges, and O. K. Andersen, Phys. Rev. Lett. **92**, 176403 (2004).

[16] L. Craco, M. S. Laad, S. Leoni, and E. Müller-Hartmann, Phys. Rev. B **70**, 195116 (2004).

[17] E. Pavarini, A. Yamasaki, J. Nuss, and O. K. Andersen, New J. Phys. **7**, 188 (2005).

[18] D. A. MacLean, H.-N. Ng, and J. Greedan, J. Solid State Chem. **30**, 35 (1979).

[19] M. Cwik, T. Lorenz, J. Baier, R. Müller, G. André, F. Bourée, F. Lichtenberg, A. Freimuth, R. Schmitz, E. Müller-Hartmann, and M. Braden, Phys. Rev. B **68**, 060401 (2003).

[20] J. M. Rondinelli and N. A. Spaldin, Adv. Mater. **23**, 3363 (2011).

[21] J. P. Perdew, K. Burke, and M. Ernzerhof, Phys. Rev. Lett. **77**, 3865 (1996).

[22] P. Giannozzi, S. Baroni, N. Bonini, M. Calandra, R. Car, C. Cavazzoni, D. Ceresoli, G. L. Chiarotti, M. Cococcioni, I. Dabo, A. D. Corso, S. de Gironcoli, S. Fabris, G. Fratesi, R. Gebauer, U. Gerstmann, C. Gougoussis, A. Kokalj, M. Lazzeri, L. Martin-Samos, N. Marzari, F. Mauri, R. Mazzarello, S. Paolini, A. Pasquarello, L. Paulatto, C. Sbraccia, S. Scandalo, G. Sclauzero, A. P. Seitsonen, A. Smogunov, P. Umari, and R. Wentzcovitch, J. Phys.: Condens. Matter **21**, 395502 (2009).

[23] D. Vanderbilt, Phys. Rev. B **41**, 7892 (1990).

[24] See Supplemental Material at http://link.aps.org/supplemental/10.1103/PhysRevB.89.161109 for further technical details.

[25] V. M. Goldschmidt, Naturwissenschaften **14**, 477 (1926).

[26] N. Marzari, A. A. Mostofi, J. R. Yates, I. Souza, and D. Vanderbilt, Rev. Mod. Phys. **84**, 1419 (2012).

[27] A. A. Mostofi, J. R. Yates, Y.-S. Lee, I. Souza, D. Vanderbilt, and N. Marzari, Comp. Phys. Comm. **178**, 685 (2008).

[28] R. Kováčik, P. Werner, K. Dymkowski, and C. Ederer, Phys. Rev. B **86**, 075130 (2012).

[29] E. Gull, A. J. Millis, A. I. Lichtenstein, A. N. Rubtsov, M. Troyer, and P. Werner, Rev. Mod. Phys. **83**, 349 (2011).

[30] M. Ferrero and O. Parcollet, TRIQS: *A Toolbox for Research in Interacting Quantum Systems*, http://ipht.cea.fr/triqs.

[31] Note that we follow the usual convention of presenting all results as a function of the intraorbital Hubbard interaction U, even though the physically relevant quantity determining the metal-insulator transition in a three-orbital model with one or two electrons is $U' - J = U - 3J$, as shown, e.g., in Ref. [36].

[32] G. Keller, K. Held, V. Eyert, D. Vollhardt, and V. I. Anisimov, Phys. Rev. B **70**, 205116 (2004).

[33] M. Jarrell and J. E. Gubernatis, Phys. Rep. **269**, 133 (1996).

[34] H. Ishida and A. Liebsch, Phys. Rev. B **77**, 115350 (2008).

[35] F. Lechermann, L. Boehnke, and D. Grieger, Phys. Rev. B **87**, 241101 (2013).

[36] P. Werner, E. Gull, and A. J. Millis, Phys. Rev. B **79**, 115119 (2009).